



Review

# Fluorination to Enhance the Tribological Properties of Carbonaceous Materials

Guillaume Haddad<sup>1,2</sup>, Nadiège Nomède-Martyr<sup>2</sup>, Philippe Bilas<sup>2,3</sup>, Katia Guérin<sup>1</sup>, Philippe Thomas<sup>2</sup>, Karl Delbé<sup>4</sup> and Marc Dubois<sup>1,\*</sup>

- <sup>1</sup> Institut de Chimie de Clermont-Ferrand (UMR 6296), Université Clermont Auvergne, Centre National de la Recherche Scientifique, BP 10448, 63000 Clermont-Ferrand, France; guillaume.haddad@uca.fr (G.H.); katia.araujo\_da\_silva@uca.fr (K.G.)
- <sup>2</sup> Groupe de Technologie des Surfaces et Interfaces (GTSI), Faculté des Sciences Exactes et Naturelles, Université des Antilles, Cedex, 97159 Pointe-à-Pitre, France; nadiège.nomède-martyr@univ-antilles.fr (N.N.-M.); philippe.bilas@univ-antilles.fr (P.B.); philippe.thomas@univ-antilles.fr (P.T.)
- <sup>3</sup> Centre Commun de Caractérisation des Matériaux des Antilles et de la Guyane, Faculté des Sciences Exactes et Naturelles, Université des Antilles, Cedex, 97159 Pointe-à-Pitre, France
- <sup>4</sup> Laboratoire Génie de Production (LGP), Université de Toulouse, INP-ENIT, 47 Avenue d'Azereix, 65000 Tarbes, France; karl.delbe@enit.fr
- \* Correspondence: marc.dubois@uca.fr

**Abstract:** This review compiles data from 77 articles on the tribological properties of fluorinated carbons CF<sub>x</sub>. Covalent grafting of fluorine atoms improves the tribological properties. The C-F bonding plays a key role in reducing friction. The tribological stability of CF<sub>x</sub>, along with their ability to form protective films from the very first cycles, provides a significant advantage in reducing wear and extending the lifespan of mechanical components. The role of the presence of fluorine atoms, their content, their distribution in the carbon lattice, and the C-F bonding, as well as the dimensionality and the size of the materials, are discussed. Some ways of improving lubrication performance and investigating friction-reducing properties and mechanisms are proposed.

**Keywords:** lubrication; tribology; tribological properties; friction; solid lubricant; fluorinated carbon; fluorinated nanocarbons; fluorination; graphite; graphene; nanotubes; diamond



Academic Editor: I. Francis Cheng

Received: 6 December 2024

Revised: 18 December 2024

Accepted: 24 December 2024

Published: 7 January 2025

**Citation:** Haddad, G.; Nomède-Martyr, N.; Bilas, P.; Guérin, K.; Thomas, P.; Delbé, K.; Dubois, M. Fluorination to Enhance the Tribological Properties of Carbonaceous Materials. *C* **2025**, *11*, 6. <https://doi.org/10.3390/c11010006>

**Copyright:** © 2025 by the authors. Licensee MDPI, Basel, Switzerland. This article is an open access article distributed under the terms and conditions of the Creative Commons Attribution (CC BY) license (<https://creativecommons.org/licenses/by/4.0/>).

## 1. Introduction

Solid lubricants are described as materials that are intentionally introduced or formed on the contact surfaces in relative motion in order to decrease friction and wear, providing protection from damage [1]. They are then widely used in modern industries such as automotive, aerospace, and aviation. Material shaping, metallurgy, and machining industries are other applications where lubrication plays a key role. Very severe operating conditions are often found, such as elevated temperatures, ultrahigh vacuum, heavy loads, extreme radiation, and chemical reactivity environments [2]. Such conditions drive the research for the development of new lubricants. Dry and chemically immobilized lubrication is expected to be an alternative to traditional wet lubricant oils. In such a context, fluorinated carbons or CF<sub>x</sub> appear as key materials. Fluorination of carbonaceous materials decreases the surface energy and reduces the micro-wear on an atomic scale. Graphite fluorides (GFs) have been well-known for a long time as excellent solid lubricants. GFs burnished on stainless-steel disks exhibit lower friction coefficients and wear than graphite and MoS<sub>2</sub>, especially at temperatures around 400 °C [3,4]. GFs exhibit extreme plasticity within lubricated contact [2]. The effect of humidity on the tribological properties of GFs is lower than

that of graphite or MoS<sub>2</sub> [2]. The oxidation in air of covalent GFs starts above about 450 °C, and low molecular weight fluorocarbons are then altered. However, fluorinated carbons cannot be applied under aqueous environments due to their high hydrophobicity. Whereas petroleum cokes have low lubricating ability, fluorinated cokes exhibit good tribological properties. Nevertheless, those properties are lower than the ones of GFs and fluorinated graphitic carbons (both with equivalent results) [5], evidencing an effect of the structural order. Those GF characteristics represent the state-of-the-art, which needs to be surpassed by taking advantage of the versatility of both the fluorination of carbonaceous (nano)materials and their exfoliation, starting with fluorinated precursors. Better-performing CF<sub>x</sub>-based solid lubricants allow severe friction conditions to be addressed. In the present review, different strategies to enhance the tribological properties of CF<sub>x</sub> will be discussed. Figure 1 summarizes most of them. The change of the fluorine content,  $x$  in CF<sub>x</sub> ( $x = \text{F/C}$  molar ratio), will be discussed first. The decrease of the stacking via exfoliation of GFs or fluorination of graphene-type materials is another route to enhance the lubricating properties as well as the use of nanometric CF<sub>x</sub>.

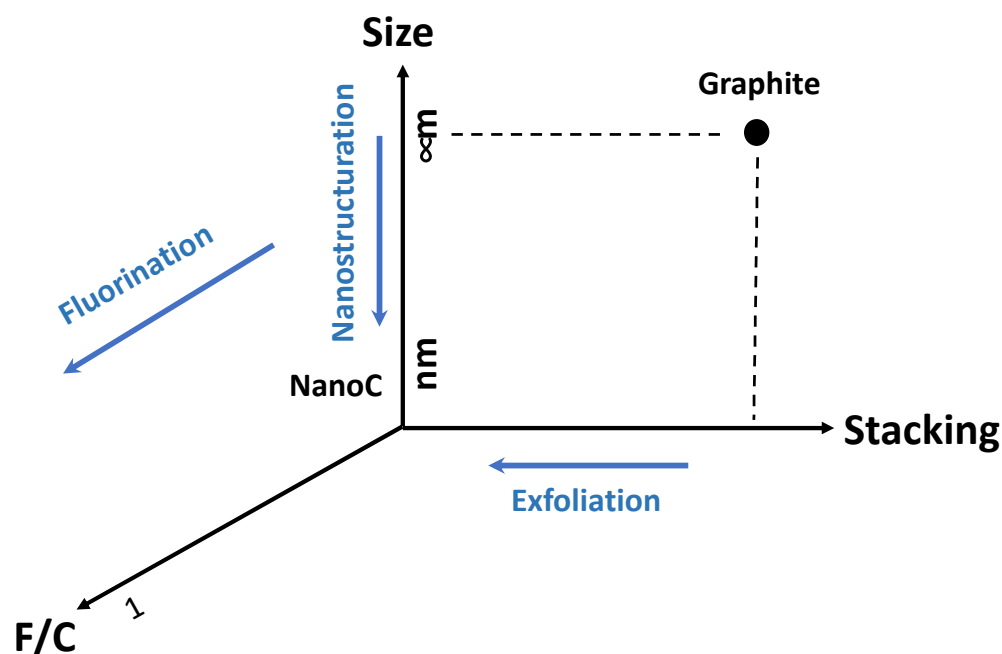


**Figure 1.** Our strategies to improve the tribological properties of fluorinated (nano)carbons.

## 2. Fluorination and Materials

The fluorination methods of porous carbons and carbonaceous fibers were recently reviewed [6,7], evidencing their versatility and the extraordinary diversity of the resulting materials. In this section, we will focus only on new developments, in particular, to prepare quasi-pure (C<sub>2</sub>F)<sub>n</sub> [8,9] and routes devoted to the preparation of solid lubricants. Table 1 gives the most significant examples. The preparation of fluorinated graphene was detailed in recent reviews [10,11]. The hydrophobic surface of CF<sub>x</sub> can be changed to add hydrophilic functionalities, e.g., with fluorinated nanotubes (CNTs), in order to increase the dispersion in water. Even with small amounts of modified F-CNTs (0.15 wt%), the tribological properties of water-based lubricants are notably enhanced with 81% and 97% decreases in friction coefficient and wear rate, respectively, compared to pure water [12].

**Table 1.** Some fluorinated carbons, their synthesis route, and fluorine content (F/C) when available.

Notation	Temperature (°C) or Method	F/C Range	Reference
(CF) <sub>n</sub>	600–650	1	[13–16]
(C <sub>2</sub> F) <sub>n</sub>	390–450	0.5	[15]
RTGF	RT followed by post-fluorination	0.4–0.9	[16,17]
Graphite fluoride	Mechanochemistry with polyethylene	0.5–0.6	[18]
Fluorinated Graphene	RT or exfoliation of (CF) <sub>n</sub>	0.05–1.0	[10,19]
F-Diamane	Exfoliation	0.5	[20]
Carbon nanofibers	380–490	0.08–1.0	[21]
Graphitized carbon blacks	340–480	0.08–0.89	[22]
Carbon Nanodiscs	280–450	0.17–0.90	[23]
F-Graphene	Activation of dormant radicals	Very low	[24]
F-Graphene	Microwave-assisted liquid-phase	0.51	[25]
F-Graphene	Ionothermal synthesis	Supposed to be 1	[26]
F-Graphene	Hydrothermal reaction with hydrofluoric and nitric acids	0.04–0.22	[27]
F-Graphene	Ultrasonication of fluorinated graphite in hydrazine hydrate		[28]
F-Graphene	Exfoliation	0.62	[29]
F-Graphene	Mechanochemistry with ammonia carbonate		[30]
Graphite fluoride-PTFE	Defluorination through gamma radiation		[31]

### 3. Tribological Properties

#### 3.1. Method

Among the different methods, the tribological properties of the (nano)carbons can be evaluated using a ball-on-plane reciprocal tribometer consisting of a steel ball (AISI 52100) rubbing against a steel plane (AISI 52100) (Figure 2). A high roughness of the plane favors the adhesion of the tested fluorinated carbons, which are deposited onto the plane. A burnishing method can be carried out; it consists of the crushing of (nano)material powder between two planes, leading to surface films of thicknesses in the 1–3 μm range. The surfaces must be then polished in order to obtain adequate roughness of both the ball and the plane, typically 20 nm and 200 nm RMS, respectively. After the application of a normal load  $F_N$ , typically of 10 N, a sliding movement is applied thanks to a tangential force  $F_T$ , which is measured with a computer-based data acquisition system. The sliding speed of the ball on the plane is fixed (e.g., 6 mm/s). Those conditions result in a contact area diameter of 140 μm and a mean contact pressure of 0.65 GPa (according to Hertz theory). The friction coefficient is defined as  $F_T/F_N$ . At the beginning of the tribological experiment, when the loaded sphere on plane contact was established, one drop of pentane (boiling point of 36.8 °C) was added in order to improve the feeding of the sliding contact with particles and then to facilitate the formation of the tribofilm. The intrinsic friction coefficients in the air of the various CF<sub>x</sub> are then measured just after pentane evaporation. Long-term experiments are necessary to evaluate the evolution of the tribological properties and quality of the tribofilms as a function of the cycle number.

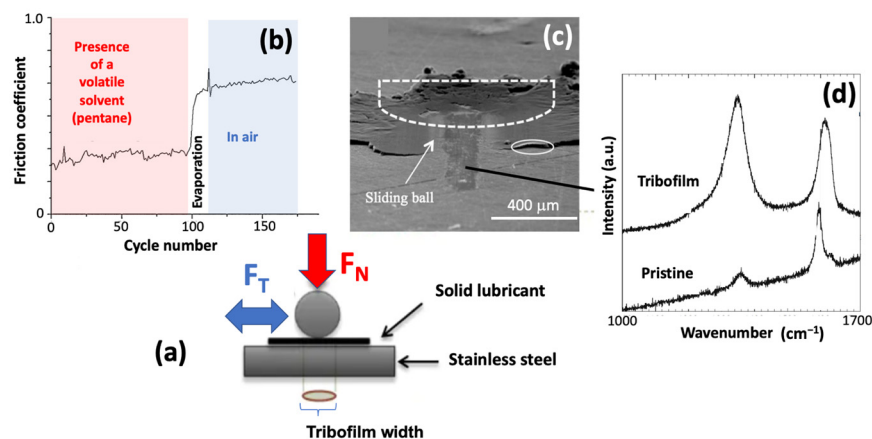


**Figure 2.** Ball-on-plane reciprocal tribometer (a) and representative examples of the evolution of the friction coefficient according to the presence of a volatile solvent (b), aspect of the wear scar obtained at 100 cycles of friction (c), and evolution of the Raman spectra during friction (d).

### 3.2. Fluorine Content

In any fluorinated carbonaceous compound, the ratios of carbon atoms to their fluorine counterparts are of utmost importance to highlight. At a given F/C molar ratio, when it is lower than 1, the distribution of F atoms must be considered. For instance, in the case of  $F/C = 0.5$ , F can be located either on the surface in a core-shell model or in the whole volume for a  $(C_2F)_n$  structural type. Watanabe et al. [13] show how specific F/C ratios need to be expressed and enunciated for all fluorinated carbon materials since the fluorine atoms change their characteristics [31,32]. Taking an example of nanometric carbons with the same F/C of 0.5, i.e., fluorinated single-walled carbon nanotubes (SWCNT), their structure was preserved up to the main composition  $CF_{0.5}$ , but the fluorination rate of SWCNT bundles was decreased with distance from the SWCNT surface to its core. It is important to note that the fluorination rate depends also on the degree of its dispersion [33]. In this section, the effect of how the fluorine content and fluorine location can drastically change the intrinsic properties of the material will be presented. To emphasize this fact, fluorinated graphitized carbon blacks (GCBs) [22] and fluorinated carbon nanofibers [21,34] are considered. As seen in Figure 3, starting at low fluorine content, fluorinated GCBs and nanofibers show quite a high friction coefficient, i.e., 0.120 and 0.138, respectively. Once further fluorinated, both exhibit lower coefficients. As the ratio of F/C increases, so do their respective friction coefficients, demonstrating the effect of fluorine content on the tribological properties of the materials. At 0.15 and 0.33 F/C ratios for fluorinated nanofibers and GCBs, respectively, the friction coefficients attain a plateau; this minimum indicates that a minimum of fluorine is needed at the surface to decrease the surface energy. As a matter of fact, the mechanism of gas/solid fluorination [32] starts on the surface, while the bulk of the material is further fluorinated when the temperature, pressure, and/or duration increases. This is further explained in literature as more thermal energy [35,36] or pressure [37] is needed to fluorinate at higher ratios, meaning more energy to fluorinate the structure of the carbon graphite. Other types of carbon materials follow this general trend about the benefits of the presence of fluorine atoms. For instance, the fluorination of silicon-containing carbon film decreases the surface energy and reduces the micro-wear on an atomic scale [38]. When compared to oxidation and nitrogen ion implantation, fluorination allows the friction coefficient of chemical-vapor-deposited diamond films to be reduced [39]. The lowest surface free energy is achieved for fluorinated diamond film.

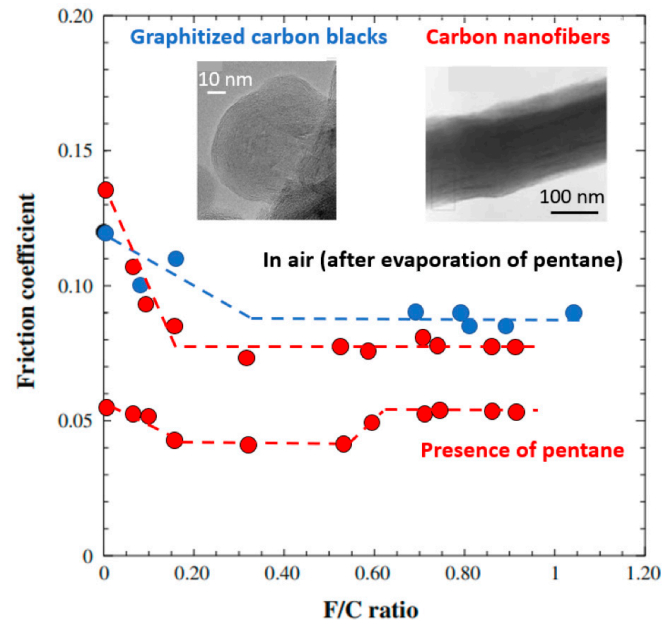


**Figure 3.** Friction coefficients of GCBs and Carbon Nanofibers.

The dependence of the friction coefficient on the F/C ratio could be more complicated. With fluorinated diamond-like carbon [40], F incorporation would be chemically beneficial because of the decrease of surface free energy and passivation of C with high energy bonds. Nevertheless, it appears structurally disadvantageous because both the carbon atomic density and H content decrease. The friction performances are more affected by humidity for fluorinated films with a low F concentration than for either highly fluorinated films (high F concentrations) or non-fluorinated films.

The case of fluorinated graphitized carbon blacks well evidences the impact of the fluorine atoms' location on the friction coefficient [22]. In order to change the thickness of the fluorinated shell around the nearly spherical core of GCBs, fluorination was performed with molecular  $F_2$  and atomic fluorine (released by the thermal decomposition of a solid fluorinating agent [6]); the processes are called direct ( $F_2$ ) and controlled ( $F\cdot$ ) fluorination, respectively. In Figure 4, the samples from two fluorination techniques have been compared to show how the type of fluorination impacts the tribological properties of the same material.

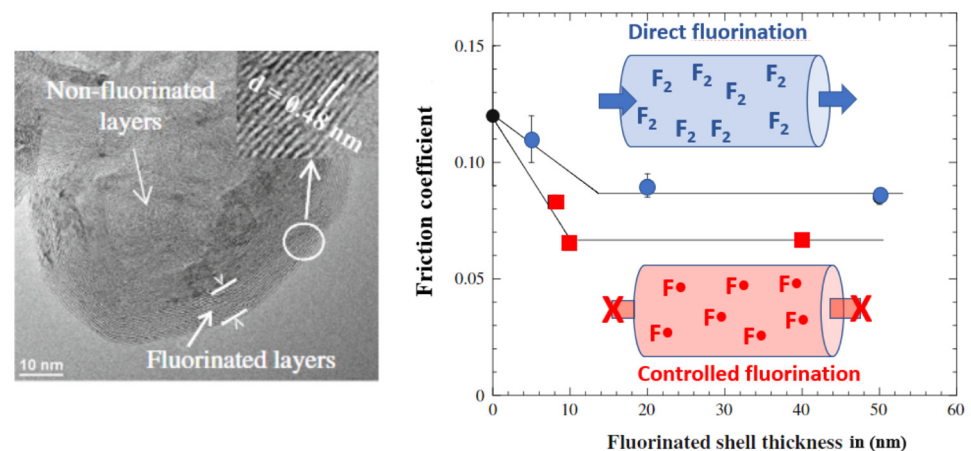


**Figure 4.** Correlation between the thickness of the fluorinated shell (obtained from TEM; a representative example is given on the left side) and friction coefficient according to the fluorination method, either with molecular fluorine (direct) or atomic fluorine (controlled). Arrows show the region of interest or magnification.

The friction coefficient changes with the thickness of the fluorinated shell. Early friction reduction mechanisms for fluorinated carbon blacks are linked to surface effects. After an initial decrease of the friction coefficient, which is due to low surface energy from the presence of F atoms, the values stabilize once the layer reaches a thickness of 12–14 nm (about 30 C-F layers for a chemical composition  $\text{CF}_{0.6}$ ). The interparticle interactions explain the differences between the samples from the two fluorination processes. At a high F/C ratio, the lower intrinsic friction coefficients for the case of controlled fluorination are explained by less delamination of the external fluorinated layers, unlike in direct fluorination, where such delamination occurs. Controlled fluorination conditions always appear milder than the use of molecular fluorine [6].

Several factors have been found to influence the friction coefficient of fluorinated diamond-like carbon films (F-DLC), i.e., the ratios of  $\text{sp}^2$  to  $\text{sp}^3$  hybridized carbons, the mechanical and chemical interaction through the ball-on-plane test, and defects either hydrogen [41] or alloy. Rubio-Roy et al. [40] analyzed the resulting materials synthesized by plasma fluorination for their response to mechanical stress. Contrary to  $\text{sp}^2$  carbon-based materials, as discussed previously, the friction coefficient increases with the fluorine content; the films exhibit a plateau at  $\text{F/C} = 0.5$ . Coupled with higher humidity, this increase is dampened, with a friction coefficient close to 0.15 at low fluorination rates. The values are even maintained at 60% and 80% humidities as the fluorination rate increases. It is theorized that humidity allows a thin layer of water molecules to be formed at the surface of the film, masking the differences and defects on the surface, while the fluorinated parts imply multiple competitive mechanisms, such as the chemical benefits of fluorine but decreasing atomic C density.

### 3.3. Effect of the Size and Dimensionality

Fluorinated carbon structures exist with different dimensionalities, and their properties are correlated directly to the size of the material used. 0D (fluorinated spherical carbon blacks) [22], 1D (fluorinated nanotubes, nanofibers) [21,42], and 2D (fluorinated graphene, fluorinated nanodiscs) [10,19,23,43,44] exist, having their own properties and applications. The fluorinated materials discussed here, i.e., 0D fluorinated spherical carbon blacks [22], 1D fluorinated nanotubes, nanofibers [21,42], and 2D fluorinated nanodiscs [23,44], exhibit similar covalent C-F bonding and closed structures at a given fluorination rate [44] that allows their tribological properties to be compared. The shape factor of fluorinated nanocarbons influences the tribological properties of the material. As shown in Figure 5, when the F/C ratio exceeds 0.15, the incorporation of fluorine atoms into the carbon lattice facilitates easy cleavage in graphitized carbon blacks (GCBs) and carbon nanofibers (CNFs). On the contrary, no improvement in friction coefficients was noted for nanodiscs after fluorination, likely due to the excellent tribological properties of the non-fluorinated initial material. The flat morphology with a large diameter/thickness ratio strongly induces an orientation of the nanodiscs parallel to the sliding surfaces. Moreover, their extended graphitic structure with a c-axis perpendicular to disc faces seems to induce easy cleavage along sliding directions parallel to the disc surfaces.

Regarding 1D with a smaller size than nanofibers, i.e., carbon nanotubes, the friction coefficients for pristine, chemically cut, and fluorinated SWNTs were found in the 0.002–0.07 range [45]. Whatever the surface chemistry, their tribological properties are partly related to the degree to which they can fill in pits and scratches and between surface asperities, etc., between sliding surfaces. Fluorination acts in two different manners: (i) mild ( $\text{C}_{20}\text{F}$  composition), it allows SWNTs bundles to be broken without significant tube wall degradation, favoring the filling of the rugosity, and (ii) more severe ( $\text{C}_2\text{F}$  and  $\text{C}_5\text{F}$ ), it

alters the graphitic quality of the tubes, leading to a poorer lubricating ability. Moreover, the highly fluorinated tubes appear less resilient towards deformation and fragile.

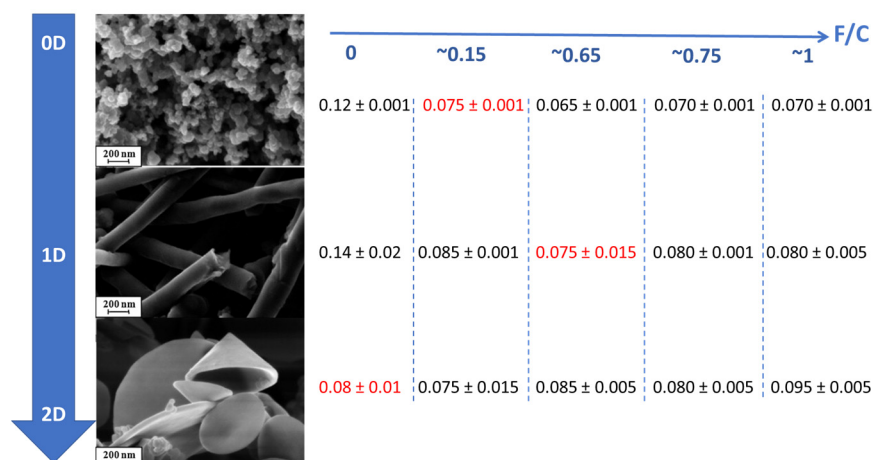


**Figure 5.** Friction coefficients of FGCs (0D), FCNFs (1D), and fluorinated nanodiscs (2D), based on the fluorination rate [44].

### 3.4. C-F Bonding

In order to evidence the effect of both the C-F bonding and the presence of the  $sp^2$  carbon phase in graphite fluoride, samples of graphite fluorinated at room temperature have been considered. Such conditions allow the fluorination to be achieved with elemental fluorine only if gaseous species are added as catalysts, i.e., HF and  $MF_n$  ( $IF_5$ ,  $BF_3$ ,  $ClF_x$ ); those gaseous fluorides are introduced either with gas or formed in situ [16]. The resulting room-temperature graphite fluorides (RTGFs) exhibit C-F bonds with weakened covalence (semi-covalent) and the maintenance of  $sp^2$  hybridization for the carbon atoms. In order to progressively convert both the C-F bonding into pure covalency and  $sp^2$  C into  $sp^3$ , a post-fluorination in pure  $F_2$  gas was performed in a wide temperature range, i.e., 150–550 °C. This is the single study in the literature about the tribological properties with progressive change in the nature of graphite fluoride from “semi-covalent” to covalent [17].

The intrinsic tribologic properties of the tested graphite fluorides clearly demonstrate that the friction reduction process is not directly related to the fluorine content or the fluorination-induced interlayer distance expansion, as the friction coefficients appear the highest for the greatest F/C ratios and interlayer distances. All the raw and post-fluorinated RTGFs present good intrinsic friction properties, better than pristine graphite (Figure 6). The lowest friction coefficients were obtained for low and intermediate post-fluorination temperatures as  $\mu$  remained in the same range of 0.055–0.06. For RTGFs post-fluorinated at temperatures higher than 450 °C, an increase of  $\mu$  was observed (0.09–0.1).

Low friction coefficients were obtained when a significant amount of graphene planes was maintained, i.e., for post-fluorination temperatures lower than 450 °C. This corresponds to partially post-fluorinated materials where graphitic domains exist, and C-F bonding is semi-covalent. The rapid increase of the friction coefficient was correlated to the increase of C-F covalency and a decrease of the graphitic domains; such characteristics have been extracted from NMR and Raman data, respectively. Regarding the changes according to the friction duration, also evidenced by Raman spectroscopy (regarding D and G bands), a partial re-building of graphitic domains occurred and resulted from C-F bond breakings induced by the friction process.

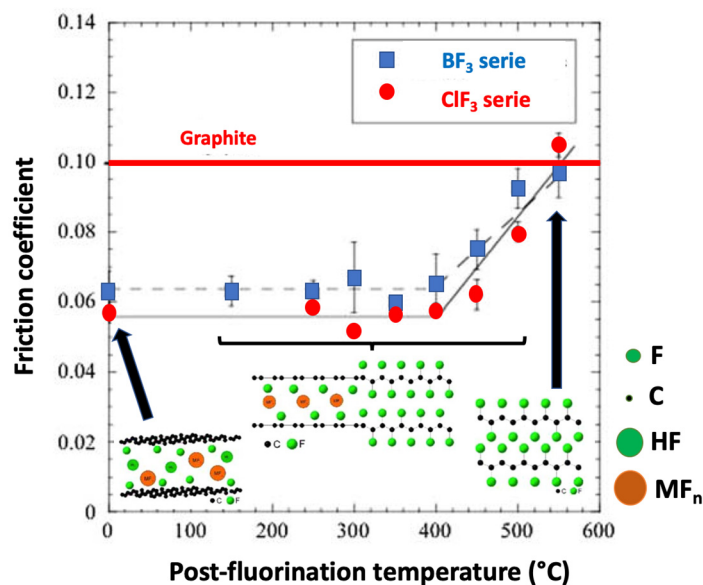


**Figure 6.** Evolution of the intrinsic friction coefficient according to the post-fluorination temperature (case of RTFs prepared with the presence of  $\text{BF}_3$  and  $\text{ClF}_3$  catalysts [17]).

Long-term friction experiments completed by Raman analyses of the tribofilms evidenced that the friction processes induced a breaking of covalent C-F bonds and a partial re-building of graphitic structure in the covalent GF (post-fluorinated at high temperature), leading to an improvement of the tribological properties of the tribofilm. In the case of semi-covalent GF (low post-treatment temperatures), the presence of intercalated fluorides and the semi-covalent C-F bonds allowed the released fluorine atoms to be trapped in the structure and/or to form new C-F bonds. The tribological performances of the tribofilm are then very stable.

### 3.5. Stacking

It is expected that the stacking of fluorinated carbons can change their friction coefficients. Fluorinated graphene [46–48] as well as fluorinated graphite both show slight variations in their characteristics. The layered structure of FG allows for effective shear between layers, promoting a low-friction environment during sliding. This mechanism is particularly beneficial in applications where sliding contact is prevalent, such as an additive to lubricants. The interlayer interactions can facilitate smooth motion. Furthermore, the  $\text{sp}^3$  hybridization from fluorine bonding introduces localized defects and functional groups, which can influence the material's mechanical properties, making it more adaptable under stress.

Extremely low surface energy and interlaminar shear strength are reached through the fluorination of carbonaceous 2D materials with low stacking, i.e., fluorographene or fluorinated graphene, either single or with few layers. The chemical interaction between the fluorocarbon sheets and steel promoted the formation of a robust tribofilm on the substrate and transfer layer on the counterpart ball, which dominantly determined the lubrication performance and wear resistance. Those benefits are perfectly evidenced by the case of fluorinated nanoflakes, which were mechanically exfoliated from a fluorinated graphite and then uniformly deposited on a stainless-steel substrate by electrophoretic deposition [49]. Excellent lubrication performances were achieved under different contact pressures, i.e., a decrease of the friction coefficient by about 54% and 66% compared to those of the pristine graphene and graphene oxide coatings, respectively.

Using fluorinated graphene obtained from the thermal exfoliation of graphite fluoride (exGF) for tribological analysis, comparing the material directly to its un-exfoliate equal is



needed. As shown in Figure 7, fluorinated graphene exhibits low variations in its friction coefficients, staying at 0.08 as the cycle number increases [19]. Exfoliation and defluorination occurred simultaneously during the thermal shock, resulting in exGF with low fluorine content, i.e., with a composition close to  $CF_{0.05}$  starting from  $CF_1$ . It is important to note that, despite the massive defluorination, the excellent lubricating performances did not deteriorate because of the weakening of the interparticle interactions due to the exfoliation process. Exfoliated structure may facilitate the formation of a homogeneous and stable tribofilm even if the fluorine content is low.

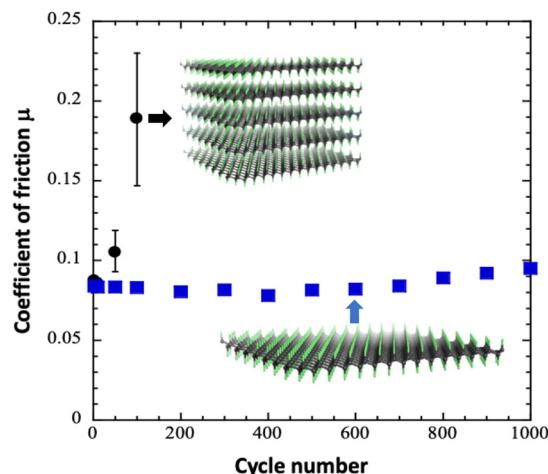


**Figure 7.** Evolution of the coefficient of friction with cycle number for raw and thermally exfoliated graphite fluoride [19].

#### 4. Mechanism for the Reduction of the Friction

The friction reduction mechanism of graphitic carbons has been generally attributed to the exfoliation of the particles and the liberation of graphitic stacks or even graphene sheets. However, the presence of intact particles in the tribofilms was noticed in different studies, as in the case of carbon nano-onions [50]. Based on the literature, it is reasonable to assume that the friction reduction mechanisms are due to direct interparticle interactions in the early stage of friction and that the carbon phases undergo structural evolution during the tribological process.

The beneficial effect of fluorination on the friction properties of graphitic carbons is underlined in Figure 8, presenting friction coefficients recorded at three cycles for pristine and fluorinated graphitized carbon blacks and carbon nanofibers. A drastic decrease of the friction coefficient is observed for the fluorinated structures due to the lowering of the surface energy of the particles, resulting in a decrease of interparticle interactions and consequently leading to an easier and more rapid formation of the tribofilms.

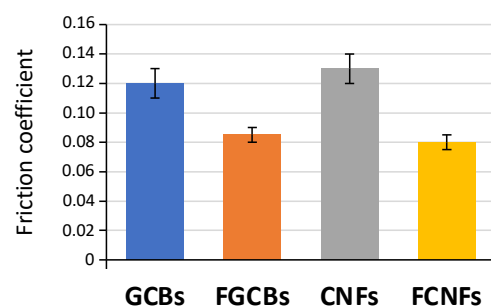


**Figure 8.** Friction coefficients recorded at three cycles for pristine and fluorinated GCBs and CNFs ( $F/C = 0.9$  for both FGCBs and FCNFs).

SEM analyses confirm that the tribofilms are composed of individual particles dispersed in a disordered matrix [22]. Raman spectroscopy appears as a powerful technique to investigate the structural evolution of the particles during the friction process. Indeed, a downshift of the D band is observed for fluorinated carbon phases compared to pristine ones. The investigation of the position of the D band of initial fluorinated carbons and associated tribofilms would, in consequence, give information about the influence of the friction process on the fluorine content. In the case of FGCBs and FCNFs, the D band is shifted towards high wave numbers during the friction experiments [21], suggesting a partial defluorination of the carbon phases. The friction coefficient remains stable during the defluorination process, indicating that the friction reduction properties are mainly due to the carbon matrix for long-term friction experiments.

The friction mechanisms are different in the case of PTFE. The friction coefficient (in the 0.2–0.3 range) is higher and depends on the sliding direction compared to PTFE bulk orientation [51]. High wear is observed. The PTFE chain undergoes scission during the friction process, creating groups ( $\text{CF}_3^+$ ,  $\text{C}_2\text{F}_5^+$ ) and fluorine ions, which react with the metallic elements of the surface to form a transfer film [52]. In the case of graphitic nanocarbons, the higher reactivity of the C-F bond and the adsorption facility of 2D carbon materials enhance their excellent intrinsic tribological properties and limit wear during the friction process.

## 5. Nano-Tribology

Several papers investigated [53,54] frictional behaviors at the nanoscale of fluorinated carbon materials thanks to Atomic Force Microscopy (AFM). Kwon et al. [55] have shown that friction on fluorinated graphene is  $\sim 6$  times larger than on pristine graphene in ultra-high vacuum and that fluorination slightly reduces the adhesion force. The total lateral stiffness recorded on fluorinated graphene was evidenced to be about five times larger than that of the pristine material [56]. Moreover, by correlating those results with molecular dynamics simulations, Li et al. [56] proposed that friction enhancement results from increased corrugation of the interfacial potential due to the strong local charge concentrated at fluorine sites. Zeng et al. [57] have focused their studies on the effect of dynamic sliding on pull-off and slide-off forces. A larger enhancement of slide-off force than the pull-off force was observed after dynamic friction sliding. This result was attributed to the coupling of dynamic tip sliding and surface energy. The wear of fluorinated graphene nanosheets deposited on silicon surfaces was investigated by Liu et al. [58], who showed that the wear resistance of FG is improved when the thickness decreases. Those results were correlated with the increase of the substrate underneath surface energy due to the interfacial charge transfer between FG and the substrate that affects the strength of FG adhesion.

Thomas et al. [21] have measured the intrinsic friction properties of fluorinated carbon nanofibers by AFM. The F/C molar ratio was 0.15 (from NMR data). TEM measurement allowed them to determine that the core was constituted of numerous randomly oriented graphitic domains, and fluorine atoms were only present in the external shell, whose thickness ranges between 30 and 40 nm. Figure 9a,b show respectively the AFM topographic image of fiber cut by FIB and the topographic profile correlated to the friction coefficient evolution as a function of sliding distance. A friction coefficient of  $0.20 \pm 0.05$  was measured for the graphitized core, whereas the friction coefficient of the fluorinated surrounding shell is  $0.35 \pm 0.05$ . The highest friction coefficient was recorded outside the fiber on the embedding resin.

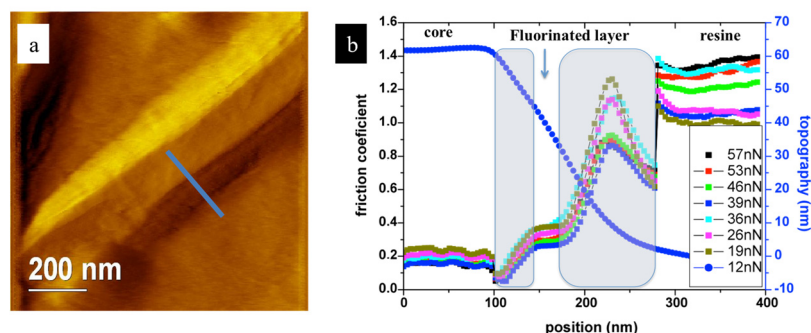


**Figure 9.** (a) Figure AFM topographic image of fiber cut by FIB, (b) topographic profile correlated to the friction coefficient evolution as a function of sliding distance.

## 6. Composites

A few composites with CF<sub>x</sub> fillers have been reported for enhancing mechanical and anti-wear properties of polymeric materials with Ultra-High-Molecular-Weight Polyethylene (UHMW-PE) [18], polyamide 66 (PA66) [59], polyimide (PI) [60] and polytetrafluoroethylene (PTFE) matrix [61]. The size and surface area of the fillers play a key role. Comparing micrometric graphite fluoride (GF) and nanometric and high surface fluorinated graphene (FG), the second gave the best results for reduction of the friction of PA66 at low concentrations (0.5 wt% into PA66), i.e., about 18% reduction in friction coefficient and about 43% reduction in wear rate when compared to the PA66 matrix. At relatively high concentrations (1.0 wt%), GF exhibited a better reinforcement effect than FG thanks to a uniform dispersion in the PA66 matrix (37% reduction in friction coefficient and 46% reduction in wear rate). Covalent bonds allow adhesion of fluorinated graphene oxide with PI matrix, resulting in enhanced mechanical and wear resistance of the nanocomposites (about 33% decrease of friction coefficient and 81% reduction of wear rate under dry friction when compared to the pure PI) [60]. The interaction between the fillers and the matrix via hydrogen bonding in the CF<sub>x</sub>-UHMW-PE composites was proposed to explain the enhancement of the tribological properties [18]. The formation of a uniform and complete transfer film on the friction interface via the tribochemical reactions results in a low friction coefficient (0.131) in PTFE/Fluorinated graphene composite [61]. Fluorinated MWCNTs have been used as additives to decrease the friction coefficient. The use of F-MWCNTs as an additive to the nanocomposite material with bismaleimide/cyanate resin allows for a decrease in wear rate since the fluorinated carbon acts as a load transfer component, thus acting upon the stiffness and toughness of nanocomposites [62].

## 7. Dispersion in Liquid Lubricating Solutions

In the presence of liquid, fluorinated carbon particles present excellent friction properties and can be used as lubricant additives. The tribological behaviors of different shapes of fluorinated nanocarbons have been investigated in the presence of pentane [44]. All the experiments show an important reduction of the friction coefficient value around 0.06, which remains stable until pentane evaporation is attributed to the simultaneous presence of the solid particles and the liquid in the sliding contact (see Figure 2). Moreover, beneficial effects on the stability of carbon particle dispersion in solvent have been demonstrated for lubrication [12,25,63–65]. Fluorinated carbon nanofibers have higher dispersion concentrations in organic solvents without surfactants. No significant modifications in their physicochemical properties upon aging have been noted. Fluorination increases the surface polarity of the carbon particles, leading to the formation of active sites for hydrogen bonding and facilitating interactions with organic molecules. Fluorinated carbon nanostructures

have been proposed as potential candidates for a new generation of friction-modifying and anti-wear additives.

Lubricating oil additives have been extensively explored for friction and wear-reduction properties. Many studies investigated the use of fluorinated carbon particles as lubricant additives. Fluorinated graphene (FG) as an additive has high efficiency due to its small size, high strength, and layered structure [26]. Ci et al. showed that a higher ratio of covalent C-F bonds improves the chemical stability of highly fluorinated reduced graphene oxide (HF-rGO), limiting the release of fluorine atoms [66]. Chen et al. showed that for the optimum addition of 1 wt% of FG in poly  $\alpha$ -olefin base oil, the average reduction of friction coefficient was 12.3%, and the wear rate decreased by 87% compared to pure PAO6 (Poly Alpha Olefin) [63]. The FG nanosheets quickly entered the sliding contact and mainly participated in the lubrication film formation. Nomede-Martyr et al. worked with fluorinated carbon nanofibers ( $CF_{0.85}$ ) and moringa oil as lubricant additives in dodecane [34]. They showed that fluorination enhanced the lubricating performances of carbon nanofibers. In the presence of  $CF_{0.85}$ , the friction coefficients are similar, whatever the percentage of moringa oil added in the blend, compared to pristine carbon nanofibers ones (Figure 10).

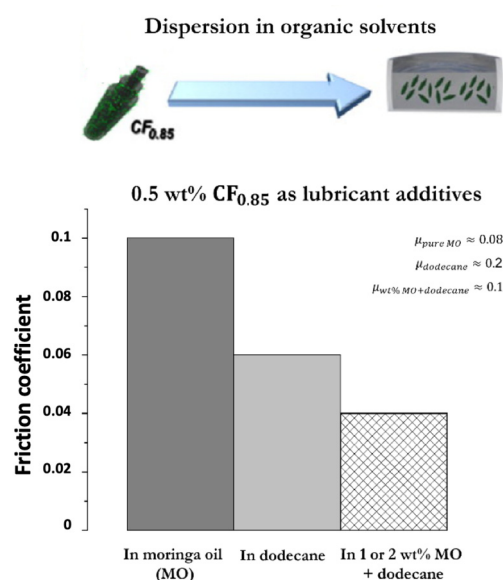


**Figure 10.** Dispersion of fluorinated nanofibers ( $CF_{0.85}$ ) in organic solvents. Friction coefficient values obtained for mixtures containing fluorinated carbon nanofibers.

For tribological applications, the introduction of functionalized groups into the carbon lattice allows such materials to be used in water-based lubricants. According to Fan et al. [24], fluorinated graphene oxide (FGO) is highly interesting for its hydrophilicity related to the amount of fluorine present on the material's surface. When used as the water lubrication additive for ceramic-steel contact, hydroxyl-modified fluorinated graphene (HOFG) can improve the pure water's load-bearing capacity significantly [25]. FGO and OHFG present better tribological properties in aqueous lubricants [25] compared to fluorinated graphene, whose dispersion in  $H_2O$  is difficult. The presence of oxygen functional groups in FGO enhances its surface interactions with lubricating fluids, promoting better dispersion and stability in aqueous environments. These oxygen groups can create a smoother and more adaptable surface, which reduces the contact area and friction between sliding surfaces. FGO coupled with acrylic acid showed those particularities due to the self-lubricating nature of the material. With  $sp^3$  hybridized carbons and an interlayer distance of around 8 Å, interlayer interactions, and stacking are made obsolete, thus managing to have a fluorinated graphene material that is both hydrophilic and has low

friction coefficients of 0.1~0.2 close to that of fluorinated graphene. Ye et al. developed a hydrophobic urea-modified fluorinated graphene (UFG) to increase the hydrophobicity of fluorinated graphene [66]. They showed a concentration of UFG aqueous dispersion of 1 mg/mL, good dispersibility in water, and the best antiwear ability with a 64% decrease in the wear rate. He et al. proposed a surfactant-assisted method to physically modify FG in order to improve its dispersibility in water [29]. They showed that 0.3 wt% of FG and 0.6 wt% of surfactant in water-based lubricant leads to over 90% reduction of friction and wear rate compared to pure water.

## 8. Conclusions and Perspectives

Throughout this review, the benefits of the tribological properties of the presence of fluorine are highlighted. The review demonstrates the crucial role of the C-F bonding and structural parameters in the tribological performances of fluorinated carbons. The semi-covalent C-F bonds play a central role in reducing friction. These bonds, which are less rigid than covalent bonds, allow a degree of flexibility in the arrangement of the graphite sheets, facilitating the formation of homogeneous transfer films on the surfaces in contact. The tribological stability of fluorocarbon compounds, combined with their ability to form protective films from the very first cycles, is a significant advantage for reducing wear and extending the life of mechanical components. Although the CF<sub>x</sub> materials reported in the literature have shown remarkable performance, it is essential to continue optimizing fluorination conditions (temperature, duration, type of catalyst). Control of these parameters would allow the properties of CF<sub>x</sub> to be customized to meet specific needs, particularly in long-term or high-load applications. Particular attention should be paid to the breaking processes of C-F bonds under tribological stress. These mechanisms play a key role in the evolution of the compounds' properties and their ability to reform aromatic structures after friction. A more detailed understanding could develop even better-performing and more durable materials.

Both the dynamic friction and the adhesive strength between the contact surfaces may be investigated using atomic force microscopy. As a representative example, the friction as a function of load exhibits a nonlinear dependence with graphene oxide, which evidences a strong adhesion. On the contrary, a linear dependence is found for the case of fluorinated graphene in accordance with weak adhesions [57].

Numerous development routes are conceivable. Among them, ultra-low friction behavior was achieved thanks to the co-doping with fluorine and sulfur of amorphous carbon films [67] some doping includes modifications of fluorinated nano-objects with H atoms [68]. Negatively charged surfaces are formed by both the delocalized  $\pi$ -system containing 'thiophene-S' and C-F bonds. The electrostatic repulsion between sliding surfaces results in low adhesion and ultra-low friction. New routes of co-doping (nano)carbons would be investigated to take benefit of the simultaneous presence of F and S, N, or B elements [69,70]. N- or S- doped nanocarbons can be used as precursors for mild fluorination; the fluorination conditions must be tailored in order to maintain S and N atoms. A gaseous mixture of F<sub>2</sub> and BF<sub>3</sub> can be used for the F and B co-doping using gas/solid fluorination of (nano)carbons.

Future developments may combine fluorinated carbons with other bidimensional materials. A synergetic effect between fluorinated graphene and MoS<sub>2</sub> nanoflakes favors excellent tribological properties with a CoF of 0.036 [71]. Both components of the nanocomposite act on the enhancements. Whereas MoS<sub>2</sub> nanoflakes provide lubrication because of the easy-shear property, the hydrophobic nature of fluorinated graphene allows the influence of external humidity on MoS<sub>2</sub> nanoflakes to be suppressed. Moreover, the formation of a tribofilm is favored, leading to a much lower friction and longer lifetime. The same

benefits were achieved with fluorinated graphene oxide nanosheets in copper metal matrix composites [72]. The formation of continuous and adhesive tribofilms at the interface, thanks to an adequate microstructure of the h-BN/graphite fluoride composites, is also at the origin of their synergistic lubrication mechanism [73]. Because of the diversity of both the shapes and dimensionalities of fluorinated nanocarbons, an ideal combination would be searched in order to amplify the synergetic effect. Numerous combinations of 2D nanomaterials, hBN, WS<sub>2</sub>, and MoS<sub>2</sub> can be considered. Fluorinated diamane (F-diamane) appears to be of great interest [74]. Diamane is a 2D structure involving only a bilayer of C with sp<sup>3</sup> hybridization over a large surface area. DFT calculations have confirmed the existence of such material, and theoretical properties calculated by PES methods show friction coefficients as low as 0.08. Fluorine atoms “passivate” the diamane sheets, enabling them to exist at ambient pressure and temperature, thus maintaining the sp<sup>3</sup> hybridization despite the metastable nature of the diamane nanosheets [75]. The tribological properties both at the micro and nanoscale are still unknown and need to be studied. Nanocomposites of F-diamane with hBN or MoS<sub>2</sub> are also promising materials for lubrication.

To the best of our knowledge, the gases emitted during lubrication with CF<sub>x</sub> are still poorly characterized, and the understanding of tribochemical mechanisms needs to be improved. This lack of knowledge is linked to the diversity of fluorinated (nano)carbons. It is important to determine whether the gases emitted belong to the per- and polyfluoroalkyl substances (PFAs) family, whose effects on the environment and human health are currently the subject of much debate. In recent years, numerous publications that reported the biological properties of PFAs and are well-reviewed in reference [76] are generally limited to perfluorooctanoic acid (PFOA) and perfluorooctane sulfonates (PFOS). Data on short-chain PFAs are much less available despite their solubility in water and the increasingly wide spectrum and volume of their use. Moreover, PFAs are being used in mixtures with varying compositions, making toxicological evaluations much more difficult. The tribometer could be coupled with gas analysis equipment such as infrared and mass spectroscopies. In a more general trend, the cytotoxicity of fluorinated (nano)carbons must be studied in the context of lubrication. Cell viability works indicated that the toxicological effects induced by the fluorinated carbons are dependent on the dose, size, shape, and fluorine content of the CF<sub>x</sub> [77]. In the same study, the authors verified that CF<sub>x</sub> has insignificant interactions with the cell viability assays.

**Author Contributions:** Conceptualization, M.D., G.H., K.G., N.N.-M., P.B., P.T., and K.D.; writing—original draft preparation, M.D., G.H., K.G., N.N.-M., P.B., K.D., P.T., and K.D.; writing—review and editing, M.D., G.H., K.G., N.N.-M., P.B., K.D., P.T., and K.D.; visualization, M.D.; supervision, M.D.; project administration, M.D. All authors have read and agreed to the published version of the manuscript.

**Funding:** The project called DIAMAT is funded by the Agence Nationale de la Recherche (ANR for the funding (PROJET N° ANR-24-CE08-1765-01)).

**Acknowledgments:** The authors (M.D., G.H., K.G., N.N.-M., P.B., P.T., and K.D) thank the ANR for the funding (PROJET N° ANR-24-CE08-1765-01).

**Conflicts of Interest:** The authors declare no conflicts of interest.

## References

1. Zhang, F.-Z.; Liu, X.-B.; Yang, C.-M.; Chen, G.-D.; Meng, Y.; Zhou, H.-B.; Zhang, S.-H. Insights into Robust Carbon Nanotubes in Tribology: From Nano to Macro. *Mater. Today* **2024**, *74*, 203–234. [[CrossRef](#)]
2. Ouyang, J.-H.; Li, Y.-F.; Zhang, Y.-Z.; Wang, Y.-M.; Wang, Y.-J. High-Temperature Solid Lubricants and Self-Lubricating Composites: A Critical Review. *Lubricants* **2022**, *10*, 177. [[CrossRef](#)]

3. Fusaro, R.L.; Sliney, H.E. *Preliminary Investigation of Graphite Fluoride (CF<sub>x</sub>)<sub>n</sub> as a Solid Lubricant*; National Aeronautics and Space Administration: Washington, DC, USA, 1969.
4. Fusaro, R.L.; Sliney, H.E. Graphite Fluoride (CF<sub>x</sub>)<sub>n</sub>—A New Solid Lubricant. *ASLE Trans.* **1970**, *13*, 56–65. [[CrossRef](#)]
5. Fusaro, R.L. Comparison of the Tribological Properties of Fluorinated Cokes and Graphites. *Tribol. Trans.* **1989**, *32*, 121–132. [[CrossRef](#)]
6. Chatenet, M.; Berthon-Fabry, S.; Ahmad, Y.; Guérin, K.; Colin, M.; Farhat, H.; Frezet, L.; Zhang, G.; Dubois, M. Fluorination and Its Effects on Electrocatalysts for Low-Temperature Fuel Cells. *Adv. Energy Mater.* **2023**, *13*, 2204304. [[CrossRef](#)]
7. Agopian, J.-C.; Téraube, O.; Charlet, K.; Dubois, M. A Review about the Fluorination and Oxyfluorination of Carbon Fibres. *J. Fluor. Chem.* **2021**, *251*, 109887. [[CrossRef](#)]
8. Lagow, R.J.; Shimp, L.A.; Lam, D.K.; Baddour, R.F. Synthesis of Poly(Carbon Monofluoride) in a Fluorine Plasma. *Inorg. Chem.* **1972**, *11*, 2568–2570. [[CrossRef](#)]
9. Watanabe, N.; Izumi, A.; Nakajima, T. Preparation of Poly-(Dicarbon Monofluoride), (C<sub>2</sub>F)<sub>n</sub> from Exfoliated Graphite. *J. Fluor. Chem.* **1981**, *18*, 475–482. [[CrossRef](#)]
10. Padamata, S.K.; Yasinskiy, A.; Stopic, S.; Friedrich, B. Fluorination of Two-Dimensional Graphene: A Review. *J. Fluor. Chem.* **2022**, *255–256*, 109964. [[CrossRef](#)]
11. Kang, W.; Li, S. Preparation of Fluorinated Graphene to Study Its Gas Sensitivity. *RSC Adv.* **2018**, *8*, 23459–23467. [[CrossRef](#)]
12. Min, C.; He, Z.; Liu, D.; Zhang, K.; Dong, C. Urea Modified Fluorinated Carbon Nanotubes: Unique Self-Dispersed Characteristic in Water and High Tribological Performance as Water-Based Lubricant Additives. *New J. Chem.* **2019**, *43*, 14684–14693. [[CrossRef](#)]
13. Watanabe, N.; Nakajima, T.; Touhara, H. *Graphite Fluorides*; Studies in Inorganic Chemistry; Elsevier Science: Burlington, VT, USA, 1988.
14. Touhara, H.; Okino, F. Property Control of Carbon Materials by Fluorination. *Carbon* **2000**, *38*, 241–267. [[CrossRef](#)]
15. Kita, Y.; Watanabe, N.; Fujii, Y. Chemical Composition and Crystal Structure of Graphite Fluoride. *J. Am. Chem. Soc.* **1979**, *101*, 3832–3841. [[CrossRef](#)]
16. Hamwi, A.; Daoud, M.; Cousseins, J.C. Graphite Fluorides Prepared at Room Temperature 1. Synthesis and Characterization. *Synth. Met.* **1988**, *26*, 89–98. [[CrossRef](#)]
17. Delbé, K.; Thomas, P.; Himmel, D.; Mansot, J.L.; Dubois, M.; Guérin, K.; Delabarre, C.; Hamwi, A. Tribological Properties of Room Temperature Fluorinated Graphite Heat-Treated Under Fluorine Atmosphere. *Tribol. Lett.* **2010**, *37*, 31–41. [[CrossRef](#)]
18. Huang, G.; Zhang, T.; Chen, Y.; Yang, F.; Huang, H.; Zhao, Y. Graphite Fluoride as a Novel Solider Lubricant Additive for Ultra-High-Molecular-Weight Polyethylene Composites with Excellent Tribological Properties. *Lubricants* **2023**, *11*, 403. [[CrossRef](#)]
19. Herraiz, M.; Dubois, M.; Batisse, N.; Petit, E.; Thomas, P. Exfoliated Fluorinated Carbons with a Low and Stable Friction Coefficient. *RSC Adv.* **2019**, *9*, 13615–13622. [[CrossRef](#)]
20. Chen, X.; Dubois, M.; Silvana Radescu, S.; Rawal, A.; Zhao, C. Liquid-phase exfoliation of F-diamane-like nanosheets. *Carbon* **2021**, *175*, 124–130. [[CrossRef](#)]
21. Thomas, P.; Himmel, D.; Mansot, J.L.; Dubois, M.; Guérin, K.; Zhang, W.; Hamwi, A. Tribological Properties of Fluorinated Carbon Nanofibres. *Tribol. Lett.* **2009**, *34*, 49–59. [[CrossRef](#)]
22. Thomas, P.; Mansot, J.L.; Molza, A.; Begarin, F.; Dubois, M.; Guérin, K. Friction Properties of Fluorinated Graphitized Carbon Blacks. *Tribol. Lett.* **2014**, *56*, 259–271. [[CrossRef](#)]
23. Thomas, P.; Himmel, D.; Mansot, J.L.; Zhang, W.; Dubois, M.; Guérin, K.; Hamwi, A. Friction Properties of Fluorinated Carbon Nanodiscs and Nanocones. *Tribol. Lett.* **2011**, *41*, 353–362. [[CrossRef](#)]
24. Fan, K.; Liu, X.; Liu, Y.; Li, Y.; Chen, Y.; Meng, Y.; Liu, X.; Feng, W.; Luo, L. Covalent Functionalization of Fluorinated Graphene through Activation of Dormant Radicals for Water-Based Lubricants. *Carbon* **2020**, *167*, 826–834. [[CrossRef](#)]
25. Ma, L.; Li, Z.; Jia, W.; Hou, K.; Wang, J.; Yang, S. Microwave-Assisted Synthesis of Hydroxyl Modified Fluorinated Graphene with High Fluorine Content and Its High Load-Bearing Capacity as Water Lubricant Additive for Ceramic/Steel Contact. *Colloids Surf. Physicochem. Eng. Asp.* **2021**, *610*, 125931. [[CrossRef](#)]
26. Min, C.; He, Z.; Song, H.; Liang, H.; Liu, D.; Dong, C.; Jia, W. Fluorinated Graphene Oxide Nanosheet: A Highly Efficient Water-Based Lubricated Additive. *Tribol. Int.* **2019**, *140*, 105867. [[CrossRef](#)]
27. Wang, D.; Jia, X.; Tian, R.; Yang, J.; Su, Y.; Song, H. Tuning Fluorine Content of Fluorinated Graphene by an Ionothermal Synthesis Method for Achieving Excellent Tribological Behaviors. *Carbon* **2024**, *218*, 118649. [[CrossRef](#)]
28. Chen, L.; Lei, J.; Wang, F.; Wang, G.; Feng, H. Facile Synthesis of Graphene Sheets from Fluorinated Graphite. *RSC Adv.* **2015**, *5*, 40148–40153. [[CrossRef](#)]
29. He, J.; Ma, L.; Yang, Y.; Jia, W.; Zhou, Q.; Yang, S.; Wang, J. Tribological Properties of Physically Modified Fluorinated Graphene and Soluble Starch Hybrid as Water-Based Lubricating Additive System. *Tribol. Int.* **2023**, *183*, 108412. [[CrossRef](#)]
30. Wan, C.; Ma, M. One-Step Exfoliation and Functionalization of Fluorinated Graphene Sheets from Fluoride Graphite by Ammonia Carbonate-Assisted Solid Ball Milling. *J. Porous Mater.* **2020**, *27*, 1319–1328. [[CrossRef](#)]

31. Singh, S.; Tyagi, M.; Tyagi, A.K.; Kaicker, P.K.; Varshney, L. Development and Characterization of Graphite Fluoride Dry Lubrication System by Using Gamma Radiation. *J. Polym. Mater.* **2020**, *36*, 305–321. [[CrossRef](#)]
32. Gupta, V.; Nakajima, T.; Ohzawa, Y.; Žemva, B. A Study on the Formation Mechanism of Graphite Fluorides by Raman Spectroscopy. *J. Fluor. Chem.* **2003**, *120*, 143–150. [[CrossRef](#)]
33. Krestinin, A.V.; Kharitonov, A.P.; Shul'ga, Y.M.; Zhigalina, O.M.; Knerel'man, E.I.; Dubois, M.; Brzhezinskaya, M.M.; Vinogradov, A.S.; Preobrazhenskii, A.B.; Zvereva, G.I.; et al. Fabrication and characterization of fluorinated single-walled carbon nanotubes. *Nanotechnol. Russ.* **2009**, *4*, 60–78. [[CrossRef](#)]
34. Nomedé-Martyr, N.; Bercion, Y.; Philippe, B.; Dubois, M.; Joseph, H.; Philippe, T. Moringa Oil With Pristine and Fluorinated Carbon Nanofibers as Additives for Lubrication. *J. Tribol.* **2021**, *144*, 051901. [[CrossRef](#)]
35. Okotrüb, A.V.; Chekhova, G.N.; Pinakov, D.V.; Yushina, I.V.; Bulusheva, L.G. Optical Absorption and Photoluminescence of Partially Fluorinated Graphite Crystallites. *Carbon* **2022**, *193*, 98–106. [[CrossRef](#)]
36. Kuriakose, A.K.; Margrave, J.L. Kinetics of the Reactions of Elemental Fluorine. IV. Fluorination of Graphite. *J. Phys. Chem.* **1965**, *69*, 2772–2775. [[CrossRef](#)]
37. Osuna, S.; Torrent-Sucarrat, M.; Solà, M.; Geerlings, P.; Ewels, C.P.; Lier, G.V. Reaction Mechanisms for Graphene and Carbon Nanotube Fluorination. *J. Phys. Chem. C* **2010**, *114*, 3340–3345. [[CrossRef](#)]
38. Miyake, S.; Kaneko, R.; Kikuya, Y.; Sugimoto, I. Micro-Tribological Studies on Fluorinated Carbon Films. *J. Tribol.* **1991**, *113*, 384–389. [[CrossRef](#)]
39. Miyake, S.; Shindo, T.; Miyake, M. Friction Properties of Surface-Modified Polished Chemical-Vapor-Deposited Diamond Films under Boundary Lubrication with Water and Poly-Alpha Olefin. *Tribol. Int.* **2016**, *102*, 287–296. [[CrossRef](#)]
40. Rubio-Roy, M.; Corbella, C.; Bertran, E.; Portal, S.; Polo, M.C.; Pascual, E.; Andújar, J.L. Effects of Environmental Conditions on Fluorinated Diamond-like Carbon Tribology. *Diam. Relat. Mater.* **2009**, *18*, 923–926. [[CrossRef](#)]
41. Sen, F.G.; Qi, Y.; Alpas, A.T. Tribology of Fluorinated Diamond-like Carbon Coatings: First Principles Calculations and Sliding Experiments. *Lubr. Sci.* **2013**, *25*, 111–121. [[CrossRef](#)]
42. Chen, X.; Li, J. Superlubricity of Carbon Nanostructures. *Carbon* **2020**, *158*, 1–23. [[CrossRef](#)]
43. Uzoma, P.C.; Hu, H.; Khadem, M.; Penkov, O.V. Tribology of 2D Nanomaterials: A Review. *Coatings* **2020**, *10*, 897. [[CrossRef](#)]
44. Nomède-Martyr, N.; Disa, E.; Thomas, P.; Romana, L.; Mansot, J.-L.; Dubois, M.; Guérin, K.; Zhang, W.; Hamwi, A. Tribological Properties of Fluorinated Nanocarbons with Different Shape Factors. *J. Fluor. Chem.* **2012**, *144*, 10–16. [[CrossRef](#)]
45. Vander Wal, R.L.; Miyoshi, K.; Street, K.W.; Tomasek, A.J.; Peng, H.; Liu, Y.; Margrave, J.L.; Khabashesku, V.N. Friction Properties of Surface-Fluorinated Carbon Nanotubes. *Wear* **2005**, *259*, 738–743. [[CrossRef](#)]
46. Şahin, H.; Topsakal, M.; Ciraci, S. Structures of Fluorinated Graphene and Their Signatures. *Phys. Rev. B* **2011**, *83*, 115432. [[CrossRef](#)]
47. Robinson, J.T.; Burgess, J.S.; Junkermeier, C.E.; Badescu, S.C.; Reinecke, T.L.; Perkins, F.K.; Zalalutdniov, M.K.; Baldwin, J.W.; Culbertson, J.C.; Sheehan, P.E.; et al. Properties of Fluorinated Graphene Films. *Nano Lett.* **2010**, *10*, 3001–3005. [[CrossRef](#)] [[PubMed](#)]
48. Feng, W.; Long, P.; Feng, Y.; Li, Y. Two-Dimensional Fluorinated Graphene: Synthesis, Structures, Properties and Applications. *Adv. Sci.* **2016**, *3*, 1500413. [[CrossRef](#)] [[PubMed](#)]
49. Liu, Y.; Li, J.; Chen, X.; Luo, J. Fluorinated Graphene: A Promising Macroscale Solid Lubricant under Various Environments. *ACS Appl. Mater. Interfaces* **2019**, *11*, 40470–40480. [[CrossRef](#)]
50. Joly-Pottuz, L.; Vacher, B.; Ohmae, N.; Martin, J.M.; Epicier, T. Anti-Wear and Friction Reducing Mechanisms of Carbon Nano-Onions as Lubricant Additives. *Tribol. Lett.* **2008**, *30*, 69–80. [[CrossRef](#)]
51. Liu, X.-X.; Li, T.-S.; Liu, X.-J.; Lv, R.-G.; Cong, P.-H. An Investigation on the Friction of Oriented Polytetrafluoroethylene (PTFE). *Wear* **2007**, *262*, 1414–1418. [[CrossRef](#)]
52. Biswas, S.K.; Vijayan, K. Friction and Wear of PTFE—A Review. *Wear* **1992**, *158*, 193–211. [[CrossRef](#)]
53. Zheng, X.; Gao, L.; Yao, Q.; Li, Q.; Zhang, M.; Xie, X.; Qiao, S.; Wang, G.; Ma, T.; Di, Z.; et al. Robust Ultra-Low-Friction State of Graphene via Moiré Superlattice Confinement. *Nat. Commun.* **2016**, *7*, 13204. [[CrossRef](#)] [[PubMed](#)]
54. Zhang, D.; Li, Z.; Klausen, L.H.; Li, Q.; Dong, M. Friction Behaviors of Two-Dimensional Materials at the Nanoscale. *Mater. Today Phys.* **2022**, *27*, 100771. [[CrossRef](#)]
55. Kwon, S.; Ko, J.-H.; Jeon, K.-J.; Kim, Y.-H.; Park, J.Y. Enhanced Nanoscale Friction on Fluorinated Graphene. *Nano Lett.* **2012**, *12*, 6043–6048. [[CrossRef](#)] [[PubMed](#)]
56. Li, Q.; Liu, X.-Z.; Kim, S.-P.; Shenoy, V.B.; Sheehan, P.E.; Robinson, J.T.; Carpick, R.W. Fluorination of Graphene Enhances Friction Due to Increased Corrugation. *Nano Lett.* **2014**, *14*, 5212–5217. [[CrossRef](#)]
57. Zeng, X.; Peng, Y.; Yu, M.; Lang, H.; Cao, X.; Zou, K. Dynamic Sliding Enhancement on the Friction and Adhesion of Graphene, Graphene Oxide, and Fluorinated Graphene. *ACS Appl. Mater. Interfaces* **2018**, *10*, 8214–8224. [[CrossRef](#)] [[PubMed](#)]
58. Liu, Y.; Jiang, Y.; Sun, J.; Wang, Y.; Qian, L.; Kim, S.H.; Chen, L. Inverse Relationship between Thickness and Wear of Fluorinated Graphene: “Thinner Is Better”. *Nano Lett.* **2022**, *22*, 6018–6025. [[CrossRef](#)] [[PubMed](#)]



59. Sun, H.; Li, T.; Lei, F.; Yang, M.; Li, D.; Huang, X.; Sun, D. Graphite Fluoride and Fluorographene as a New Class of Solid Lubricant Additives for High-performance Polyamide 66 Composites with Excellent Mechanical and Tribological Properties. *Polym. Int.* **2020**, *69*, 457–466. [[CrossRef](#)]
60. Min, C.; He, Z.; Liang, H.; Liu, D.; Dong, C.; Song, H.; Huang, Y. High Mechanical and Tribological Performance of Polyimide Nanocomposite Reinforced by Fluorinated Graphene Oxide. *Polym. Compos.* **2020**, *41*, 1624–1635. [[CrossRef](#)]
61. Liang, L.; Song, L.; Yang, Y.; Li, F.; Ma, Y. Tribological Properties of Polytetrafluoroethylene Improved by Incorporation of Fluorinated Graphene with Various Fluorine/Carbon Ratios Under Dry Sliding Condition. *Tribol. Lett.* **2021**, *69*, 21. [[CrossRef](#)]
62. Li, P.; Li, T.; Yan, H. Mechanical, Tribological and Heat Resistant Properties of Fluorinated Multi-Walled Carbon Nanotube/Bismaleimide/Cyanate Resin Nanocomposites. *J. Mater. Sci. Technol.* **2017**, *33*, 1182–1186. [[CrossRef](#)]
63. Chen, Y.; Hu, E.; Zhong, H.; Wang, J.; Subedi, A.; Hu, K.; Hu, X. Characterization and Tribological Performances of Graphene and Fluorinated Graphene Particles in PAO. *Nanomaterials* **2021**, *11*, 2126. [[CrossRef](#)] [[PubMed](#)]
64. Konios, D.; Stylianakis, M.M.; Stratakis, E.; Kymakis, E. Dispersion Behaviour of Graphene Oxide and Reduced Graphene Oxide. *J. Colloid Interface Sci.* **2014**, *430*, 108–112. [[CrossRef](#)] [[PubMed](#)]
65. Ci, X.; Zhao, W.; Luo, J.; Wu, Y.; Ge, T.; Xue, Q.; Gao, X.; Fang, Z. How the Fluorographene Replaced Graphene as Nanoadditive for Improving Tribological Performances of GTL-8 Based Lubricant Oil. *Friction* **2021**, *9*, 488–501. [[CrossRef](#)]
66. Ye, X.; Ma, L.; Yang, Z.; Wang, J.; Wang, H.; Yang, S. Covalent Functionalization of Fluorinated Graphene and Subsequent Application as Water-based Lubricant. *ACS Appl. Mater. Interfaces* **2016**, *8*, 7483–7488. [[CrossRef](#)]
67. Wang, F.; Wang, L.; Xue, Q. Fluorine and Sulfur Co-Doped Amorphous Carbon Films to Achieve Ultra-Low Friction under High Vacuum. *Carbon* **2016**, *96*, 411–420. [[CrossRef](#)]
68. Qiang, L.; Zhang, B.; Gao, K.; Gong, Z.; Zhang, J. Hydrophobic, Mechanical, and Tribological Properties of Fluorine Incorporated Hydrogenated Fullerene-like Carbon Films. *Friction* **2013**, *1*, 350–358. [[CrossRef](#)]
69. Salpekar, D.; Serles, P.; Colas, G.; Ma, L.; Yadav, S.; Hamidinejad, M.; Khabashesku, V.N.; Gao, G.; Swaminathan, V.; Vajtai, R.; et al. Multifunctional Applications Enabled by Fluorination of Hexagonal Boron Nitride. *Small* **2024**, 2311836. [[CrossRef](#)]
70. Sun, J.; Du, S. Application of Graphene Derivatives and Their Nanocomposites in Tribology and Lubrication: A Review. *RSC Adv.* **2019**, *9*, 40642–40661. [[CrossRef](#)] [[PubMed](#)]
71. Liu, Y.; Li, J.; Yi, S.; Ge, X.; Chen, X.; Luo, J. Enhancement of Friction Performance of Fluorinated Graphene and Molybdenum Disulfide Coating by Microdimple Arrays. *Carbon* **2020**, *167*, 122–131. [[CrossRef](#)]
72. Savjani, N.; Mercadillo, V.O.; Hodgeman, D.; Paterakis, G.; Deng, Y.; Vallés, C.; Anagnostopoulos, G.; Galiotis, C.; Bissett, M.A.; Kinloch, I.A. Tribology of Copper Metal Matrix Composites Reinforced with Fluorinated Graphene Oxide Nanosheets: Implications for Solid Lubricants in Mechanical Switches. *ACS Appl. Nano Mater.* **2023**, *6*, 8202–8213. [[CrossRef](#)] [[PubMed](#)]
73. Fusaro, R.L.; Sliney, H.E. Lubricating Characteristics of Polyimide Bonded Graphite Fluoride and Polyimide Thin Films. *E Trans.* **1973**, *16*, 189–196. [[CrossRef](#)]
74. Wang, J.; Li, L.; Wang, J.; Yang, W.; Guo, P.; Li, M.; Liu, D.; Zeng, H.; Zhao, B. First-Principles Study on the Nanofriction Properties of Diamane: The Thinnest Diamond Film. *Nanomaterials* **2022**, *12*, 2939. [[CrossRef](#)] [[PubMed](#)]
75. Bakharev, P.V.; Huang, M.; Saxena, M.; Lee, S.W.; Joo, S.H.; Park, S.O.; Dong, J.; Camacho-Mojica, D.C.; Jin, S.; Kwon, Y.; et al. Chemically Induced Transformation of Chemical Vapour Deposition Grown Bilayer Graphene into Fluorinated Single-Layer Diamond. *Nat. Nanotechnol.* **2020**, *15*, 59–66. [[CrossRef](#)] [[PubMed](#)]
76. Stahl, T.; Mattern, D.; Brunn, H. Toxicology of perfluorinated compounds. *Environ. Sci. Eur.* **2011**, *23*, 38. [[CrossRef](#)]
77. Teo, W.Z.; Chua, C.K.; Sofer, Z.; Pumera, M. Fluorinated Nanocarbons Cytotoxicity. *Chem.—Eur. J.* **2015**, *21*, 13020–13026. [[CrossRef](#)] [[PubMed](#)]

**Disclaimer/Publisher’s Note:** The statements, opinions and data contained in all publications are solely those of the individual author(s) and contributor(s) and not of MDPI and/or the editor(s). MDPI and/or the editor(s) disclaim responsibility for any injury to people or property resulting from any ideas, methods, instructions or products referred to in the content.